Non-Abelian Braiding of Light

Thomas Iadecola, Thomas Schuster, and Claudio Chamon

Phys. Rev. Lett. **117**, 073901 — Published 10 August 2016

DOI: 10.1103/PhysRevLett.117.073901

Non-Abelian braiding of light

Thomas Iadecola, Thomas Schuster, and Claudio Chamon
Physics Department, Boston University, Boston, Massachusetts 02215, USA
(Dated: July 27, 2016)

Many topological phenomena first proposed and observed in the context of electrons in solids have recently found counterparts in photonic and acoustic systems. In this work, we demonstrate that non-Abelian Berry phases can arise when coherent states of light are injected into "topological guided modes" in specially-fabricated photonic waveguide arrays. These modes are photonic analogues of topological zero modes in electronic systems. Light traveling inside spatially well-separated topological guided modes can be braided, leading to the accumulation of non-Abelian phases, which depend on the order in which the guided beams are wound around one another. Notably, these effects survive the limit of large photon occupation, and can thus also be understood as wave phenomena arising directly from Maxwell's equations, without resorting to the quantization of light. We propose an optical interference experiment as a direct probe of this non-Abelian braiding of light.

Manifestations of topology in physical systems, specifically in the form of so-called geometric phases, [1, 2] have risen to prominence over the last three decades. Geometric phases were shown by M.V. Berry to arise in quantum systems under cyclic adiabatic variation of parameters, [2] but it was later understood [3] that this phase had been discovered thirty years earlier in the context of classical optics by S. Pancharatnam. [1] The close analogy between quantum mechanics and classical optics has remained over the years, and many of the striking topological states of matter associated with electrons in solids, such as topological insulators and semimetals, [4] have recently found counterparts in photonic [5–13] and acoustic [14–19] systems. The present work aims to further highlight and deepen the connection between topological phenomena in solids and in classical wave mechanics by demonstrating a new facet to this correspondence. We demonstrate the existence of a classical analogue of the *non-Abelian* Berry phase [20] that arises from "braiding" topological defects in solids.

One route to non-Abelian Berry phases in electronic systems lies in the remarkable physics of zero modes. As was pointed out in pioneering work by R. Jackiw with C. Rebbi [21] and P. Rossi, [22] localized zero-energy fermionic states can bind to topological defects in an order parameter, such as kinks in one dimension and vortices in two dimensions. In systems where electric charge is a good quantum number, these zero modes carry charges that are fractions of the "fundamental" electron charge. [21, 23, 24] In chiral superconductors, where charge conservation is broken, these localized modes are Majorana bound states with non-Abelian statistics. [22, 25–27] At the mean-field level, where interactions between electrons are neglected, this non-Abelian statistcs can be understood in terms of the accumulation of non-Abelian Berry phases as defects are adiabatically exchanged with one another. [28] The non-Abelian nature of this process manifests itself in dependence of these phases on the order in which the defects are interchanged, in contrast to the usual "Abelian" Berry phase.

In this paper, we propose a novel means of realizing topological zero modes in photonic, rather than electronic, systems, and demonstrating their non-Abelian braiding directly. The proposed realization consists of non-interacting photons propagating in the non-trivial background of a photonic lattice with topological defects whose positions are controllable. Light channeled into "topological guided modes" localized at these defects can be braided, leading to the accumulation of non-Abelian phases that depend on the order in which the braids occur. We demonstrate that this effect manifests itself at both the quantum and classical levels, owing to the linearity of the equations of motion for noninteracting light.

The zero modes we propose to realize are photonic analogues of Kekulé zero modes in graphene, [24] which are bound to vortices in the complex order parameter $\Delta(\boldsymbol{r})$ describing a dimerization pattern in the hexagonal lattice (Fig. 1). The translation between electrons and photons is achieved by replacing the sites of the lattice with waveguides embedded in a bulk optical medium (*e.g.* fused silica), [29] which are extended in the z direction and whose x-y positions mimic the 2D positions of the carbon atoms in the distorted graphene lattice. The wave equation for the paraxial propagation of light in such a waveguide array maps directly onto the time-dependent Schrödinger equation (SE), where the time coordinate t in the SE is replaced by the coordinate z along the direction of light propagation. This wave equation can be further mapped, using coupled mode theory, [30] to a linear differential equation that is in one-to-one correspondence with the noninteracting tight-binding model of the electronic system. The waveguides themselves can therefore be thought of as the world lines of the carbon atoms, with straight waveg-

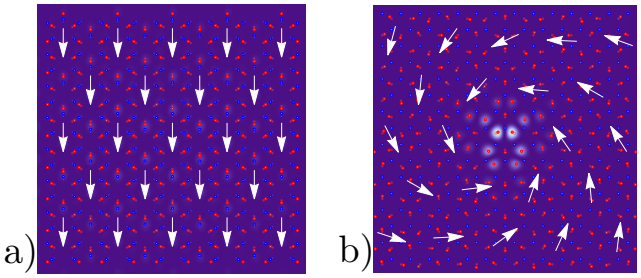

FIG. 1: a) Uniform Kekulé distortion in a hexagonal waveguide lattice at a slice of constant z. The faint circles represent the original hexagonal lattice, while darker circles represent the distorted lattice. Sublattice A is colored red, while sublattice B is colored blue. The overlaid vector field represents the magnitude and direction of the order parameter $\Delta(\boldsymbol{r})$. The background is an image of a low-lying eigenmode of Eq. (1). The intensity pattern represents the amplitude of the electric field in each waveguide. b) Waveguide lattice in the presence of a vortex in the Kekulé pattern, with an overlaid order-parameter vector field showing circulation around the vortex core. The background is an intensity plot of the localized zero-mode wavefunction. We have chosen a vortex profile in which only sublattice A is displaced.

uides corresponding to a lattice that is static in time.

Waveguide arrays of this type have been realized, written into bulk materials with exquisite precision using femtosecond lasers, [31] (see Ref. 29 for a review). They have been used to mimic graphene and other electronic systems with both static lattices [5, 32–34] and ones that change as a function of time. [10, 11] The experimental protocol suggested here hinges on this capability to execute a braiding procedure in which three vortices are wound around one another. As we show below, a protocol can be chosen that reveals the non-Abelian nature of the braiding directly via interference between different braiding patterns.

Our starting point is the coupled-mode equation for paraxial light propagation through the waveguide array,

$$i\,\partial_z\,\psi_{\boldsymbol{r}}(z) = \sum_{j=1}^{3} H_{\boldsymbol{r},\boldsymbol{r}\pm\boldsymbol{s}_j}\,\psi_{\boldsymbol{r}\pm\boldsymbol{s}_j}(z). \qquad (1)$$

Here, the vector $\boldsymbol{r}$ is defined on a hexagonal lattice divided into two triangular sublattices that we call A and B. The vectors $+\boldsymbol{s}_j$ (j=1,2,3) connect the point $\boldsymbol{r}$ in sublattice A to its three nearest neighbors in sublattice B, located a distance a away, and $-\boldsymbol{s}_j$ connect points in B to their neighbors in A. For simplicity, we assume the light in the array to be monochromatic, so that Eq. (1) is frequency-independent. Eq. (1) is formally identical to a noninteracting tight-binding model in which the time coordinate t has been replaced by the longitudinal coordinate z. Its solutions can be decomposed into eigenmodes $\psi_{\nu,\boldsymbol{r}}(z) = \psi_{\nu,\boldsymbol{r}}\,e^{-i\kappa_\nu z}$, where $\nu = 0,\ldots,2N-1$, with N the number of unit cells in the waveguide array, labels the "energy eigenvalues" κ_ν. The "wavefunction" $\psi_{\boldsymbol{r}}(z)$ in Eq. (1) is related to the amplitude of the local electric field $\boldsymbol{E}_{\boldsymbol{r}}(z,t)$ on the "site" $\boldsymbol{r}$. It is useful to work with the *quantized* electric field operator[35]

$$\hat{\boldsymbol{E}}_{\boldsymbol{r}}(z,t) = \sum_{\nu} \psi_{\nu,\boldsymbol{r}}\,e^{i[(k_\omega-\kappa_\nu)z-\omega t]}\,\hat{b}_\nu\,\boldsymbol{n} + \text{H.c.} \qquad (2)$$

where $\boldsymbol{n}$ is a unit vector in the x-y plane describing the polarization of the field and k_ω satisfies the dispersion relation of a single waveguide. The ladder operators $\hat{b}_\nu$ satisfy the bosonic commutation relations $[\hat{b}_\nu, \hat{b}^\dagger_{\nu'}] = \delta_{\nu,\nu'}$. [See Supplemental Material (SM) for details on the quantization procedure.]

The "Hamiltonian" in Eq. (1) depends exponentially on distances between nearest-neighbor waveguides (we neglect longer-range couplings for the moment). We take $H_{\boldsymbol{r},\boldsymbol{r}+\boldsymbol{s}_j} = -t - \delta t_{\boldsymbol{r},j}$, where $\delta t_{\boldsymbol{r},j} = \Delta(\boldsymbol{r})\,e^{i\boldsymbol{K}_+\cdot\boldsymbol{s}_j}\,e^{2i\boldsymbol{K}_+\cdot\boldsymbol{r}}/2 + \text{c.c.}$ (we denote by $\boldsymbol{K}_\pm$ the locations of the two inequivalent Dirac points, at opposite corners of the hexagonal Brillouin zone). Here, the parameter t describes the evanescent couplings of the waveguides, and the position-dependent function $\delta t_{\boldsymbol{r},j}$ describes modulations of these couplings due to displacements of the waveguides from their original x-y positions. The complex-valued Kekulé order parameter $\Delta(\boldsymbol{r})$ controls the distortion of the lattice. [24] A vortex in $\Delta(\boldsymbol{r})$ is a defect in this distortion pattern, but not the lattice itself. The order parameter in the presence of a single vortex centered at the origin reads $\Delta(\boldsymbol{r}) = \Delta_0(r)\,e^{i(\alpha-\theta)}$ in polar coordinates $\boldsymbol{r} = (r,\theta)$. Here, $\Delta_0(r) = \Delta\,\tanh(r/\ell_0)$ describes the spatial profile of the vortex, which has a core radius ℓ_0, and α is the phase of the order parameter.

The zero mode in the presence of this vortex profile can be found by setting the left-hand side of Eq. (1) to zero and solving for $\psi_{\boldsymbol{r}}$. The zero-mode solution is tightly localized near the core of the vortex, with a size of order $1/\Delta$, and has support on sublattice A only [see Fig. 1(B)]. [If we send $\theta \to -\theta$ in $\Delta(\boldsymbol{r})$, the zero mode has support on sublattice B instead. [24]] This means that light propagating in the zero mode travels as if confined to an "optical fiber" located at the vortex core, albeit with evanescent decay into neighboring waveguides in the same sublattice. However, the zero mode differs crucially from a mode in an optical fiber, both because it takes the distortion of an entire waveguide lattice to create, and because it depends on the topological nature of this distortion. These "topological guided modes" are responsible for the non-Abelian effects described below.

The above discussion neglects the presence of various lattice effects that can shift the zero mode eigenvalue to a finite momentum. In principle, this makes possible the accumulation of path-dependent (*i.e.* non-topological)

dynamical phases during braiding. However, as we show in detail in the SM, these effects can be neglected to resonable precision without fine-tuning. There, we estimate (conservatively) that we can perform thousands of braids before the effects of dynamical phases begin to manifest themselves.

To facilitate our discussion of the non-Abelian braiding of vortices like the one above, we work in the continuum limit, where the analytical form of the vortex wavefunction is known. (Exact diagonalization calculations corroborating these results are reviewed in the SM.) On length scales much longer than a, the operator that annihilates a photon in the zero mode is

$$\hat{b}_0 = \int \mathrm{d}\boldsymbol{r} \left[u(\boldsymbol{r})\, \hat{b}_+(\boldsymbol{r}) + u^*(\boldsymbol{r})\, \hat{b}_-(\boldsymbol{r}) \right] , \qquad (3)$$

where $\hat{b}_\pm(\boldsymbol{r})$ annihilate a photon at the Dirac points $\boldsymbol{K}_\pm$. (These operators are assumed to be normalized such that the canonical commutation relation $[\hat{b}_0, \hat{b}_0^\dagger] = 1$ holds.) The function $u(\boldsymbol{r}) \equiv u(r)$ is given, up to normalization, by [24]

$$u(r) = e^{i(\alpha/2+\pi/4)}\, e^{-\int_0^r \mathrm{d}r'\, \Delta_0(r')}. \qquad (4)$$

Note that the zero mode amplitude $u(r)$ is *double-valued*: when α, the phase of the order parameter $\Delta(\boldsymbol{r})$, changes by 2π, $u(r)$ acquires a minus sign. The origin of this double-valuedness lies in the fact that $u(r)$ is a solution to the Dirac equation, and therefore must transform as a spinor under changes in α.

The quantum states created by $\hat{b}_0^\dagger$ can be connected to the macroscopic state of light in the waveguide array by defining the coherent state

$$|\lambda\rangle = e^{-|\lambda|^2/2}\, e^{\lambda \hat{b}_0^\dagger} |0\rangle \qquad (5)$$

with mean photon number $\langle \hat{b}_0^\dagger \hat{b}_0 \rangle = |\lambda|^2$. These states provide a faithful description of the electric field in the waveguide array in the large-$|\lambda|$ limit when the input light is a coherent, monochromatic laser spot centered on the vortex core. In this case, the contribution of the photonic zero mode to the classical electric field is given by [c.f. Eq. (2)]

$$\boldsymbol{E}_{0,\boldsymbol{r}}(z,t) = \lambda\, u(r)\, e^{i(\boldsymbol{K}_+ \cdot \boldsymbol{r} + k_\omega\, z - \omega t)}\, \boldsymbol{n} + \text{c.c.}, \qquad (6)$$

with $u(r)$ given in Eq. (4) and λ defined by Eq. (5). The ease with which one can translate between the quantum and classical descriptions of the waveguide array owes to the fact that photons in the array are noninteracting. Indeed, an alternative way of deriving Eq. (6) is to solve Maxwell's equations directly in the presence of a vortex.

Let us now study the braiding of zero modes in an infinite system with v vortices at *z-dependent* positions $\boldsymbol{R}_i(z)$ $(i = 1, \ldots, v)$. The order parameter in the presence of this vortex configuration is given by

$$\Delta(\boldsymbol{r}) = \Delta \prod_{j=1}^{n} \tanh(|\boldsymbol{r} - \boldsymbol{R}_j|/\ell_0)\, e^{i[\alpha_j - \arg(\boldsymbol{r} - \boldsymbol{R}_j)]} , \quad (7)$$

and the zero-mode Hilbert space is spanned by the operators $\hat{b}_{0,i}^\dagger$. A clockwise adiabatic exchange of vortices i and $i+1$ is implemented by winding the vortex-core coordinates $\boldsymbol{R}_i(z)$ and $\boldsymbol{R}_{i+1}(z)$ around one another as functions of increasing z (see, e.g., the braids in Fig. 2). In the SM, we show that the nontrivial nature of this winding process stems from the double-valuedness of $u(r)$ under $\alpha \to \alpha - 2\pi$. (We verified this statement for the zero-mode wavefunction on the lattice via a numerical tight-binding calculation, as we describe in the SM.) The effect of this exchange, up to a gauge choice, is to map $\hat{b}_{0,i}^\dagger \to \hat{b}_{0,i+1}^\dagger$ and $\hat{b}_{0,i+1}^\dagger \to -\hat{b}_{0,i}^\dagger$ while leaving all other vortex operators unchanged, similarly to the case of Majorana [26] and Dirac zero modes [36] in electronic systems. The operator that implements this exchange is

$$\hat{\tau}_i = e^{\pi\, (\hat{b}_{0,i+1}^\dagger \hat{b}_{0,i} - \hat{b}_{0,i}^\dagger \hat{b}_{0,i+1})/2}. \qquad (8)$$

One verifies by direct calculation that these operators satisfy $[\hat{\tau}_i, \hat{\tau}_j] = 0$ for $|i-j| > 1$ and $\hat{\tau}_i \hat{\tau}_j \hat{\tau}_i = \hat{\tau}_j \hat{\tau}_i \hat{\tau}_j$ for $|i-j| = 1$, and therefore form a unitary representation of $\mathcal{B}_v$, the braid group on v strands. [37] The action of these generators on a state

$$|n_1, \ldots, n_v\rangle = \prod_{i=1}^{v} \frac{(\hat{b}_{0,i}^\dagger)^{n_i}}{\sqrt{n_i!}} |0\rangle, \qquad (9)$$

representing a system with v vortices, each with a fixed number of photons, is given by

$$\hat{\tau}_i\, |\ldots, n_i, n_{i+1}, \ldots\rangle = (-1)^{n_{i+1}} |\ldots, n_{i+1}, n_i, \ldots\rangle. \quad (10)$$

We now explain the consequences of the above phase factor, which arises purely from braiding the vortices. Consider the case of two vortices, and the operation of winding one around the other, which restores them to their initial locations. We begin by considering i) an example where this phase factor does not lead to unitary operations on a multi-dimensional space of degenerate states, and then turn to ii) an example where it does. For case i), consider any eigenstate of occupation number, $|n_1, n_2\rangle$, which upon winding goes to the state $(-1)^{n_1+n_2} |n_1, n_2\rangle$; clearly, the initial and final states are equal up to a phase, and the braiding operation acts on a one-dimensional space only. In contrast, consider case ii), where we take an initial state that is not an eigenstate of occupation number, but rather a superposition

of states with occupation 0 and 1, for example. Then winding takes

$$\frac{|0\rangle+|1\rangle}{\sqrt{2}} \otimes \frac{|0\rangle+|1\rangle}{\sqrt{2}} \longrightarrow \frac{|0\rangle-|1\rangle}{\sqrt{2}} \otimes \frac{|0\rangle-|1\rangle}{\sqrt{2}} \,. \qquad (11)$$

Clearly, the initial and final states are different (here, they are orthogonal). This is a crucial hallmark of the non-Abelian nature of the action of the braiding generators on these states. Thus, the essential ingredient necessary for braiding to connect states in a multi-dimensional Hilbert space is that the initial state of the zero mode system consists of superpositions of states with even and odd numbers of photons.

Such superpositions do not only exist within the domain of quantum optics. The coherent states defined in Eq. (5) consist of a superposition of photon states with *all* occupation numbers, and can be created by shining a coherent laser beam centered on a single vortex core. Let us now consider a system of v vortices, into each of which is loaded a coherent state of photons:

$$|\lambda_1, \ldots, \lambda_v\rangle = \prod_{i=1}^{v} e^{-|\lambda_i|^2/2}\, e^{\lambda_i \hat{b}^\dagger_{0,i}}\, |0\rangle. \qquad (12)$$

The action of the braiding generators on these states is found from Eq. (10) to be

$$\hat{\tau}_i |\ldots, \lambda_i, \lambda_{i+1}, \ldots\rangle = |\ldots, -\lambda_{i+1}, \lambda_i, \ldots\rangle. \qquad (13)$$

To see that this braiding operation connects quantum states in a multi-dimensional space of degenerate states, consider again the winding of two vortices, which restores their initial locations. For a coherent state, this operation takes

$$|\lambda_1, \lambda_2\rangle \longrightarrow |-\lambda_1, -\lambda_2\rangle \,. \qquad (14)$$

The overlap of these two states is $\langle \lambda_1, \lambda_2 | -\lambda_1, -\lambda_2\rangle = e^{-2(|\lambda_1|^2+|\lambda_2|^2)}$, whose magnitude is smaller than one, indicating that the states are linearly independent. This demonstrates that the Hilbert space spanned by the braiding operations is multi-dimensional. Moreover, in the limit where a large number of photons are loaded into the zero modes (large $|\lambda_{1,2}|$, which is to be expected from a laser), the overlap is exponentially small, and the initial and final states become orthogonal.

At this point, it is worthwhile to reflect on the significance of the fact that the effect of braiding the vortices manifests itself at the level of coherent states, which are essentially classical. While the braiding of these vortices can be understood at the quantum (*i.e.* few-photon) level, its effects permeate the entire zero-mode Hilbert space for arbitrary occupation numbers. Consequently, the quantum action of the braiding generators survives the limit of large occupations, so that macroscopic effects of this braiding can be seen. In particular, observe that $\lambda_i \to -\lambda_i$ under a braid corresponds, in the limit of large $|\lambda_i|$, to a change in the sign of the electric field $\boldsymbol{E}_i$ near the core of the ith vortex [c.f. Eq. (6)]. This observation forms the basis of our discussion below.

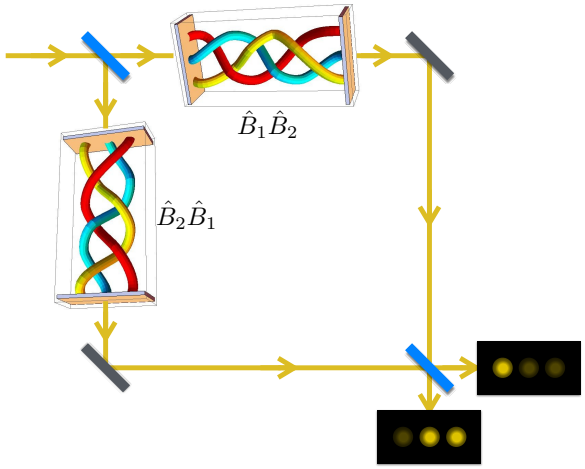

FIG. 2: Schematic of the proposed photonic non-Abelian interferometer. A coherent laser beam (one of three, one for each vortex in a lattice) passes through a 50/50 beam splitter (blue) and simultaneously enters two separate photonic lattices fabricated with the two braids to be compared. The two output beams are reflected by mirrors (grey) into another beam splitter that interferes the two signals and outputs the sum and difference to separate screens (black). For the choice of braids used here, one screen shows a bright and two dark spots, while the other screen shows the "logical complement" of the first, with one dark and two bright spots.

We now propose an experiment that could provide direct and unambiguous evidence for non-Abelian braiding at the level of coherent states. The photonic non-Abelian interferometer (PNAI) that we propose, shown in Fig. 2, consists of two separate photonic lattices, each with three vortices, with waveguides written into the host medium in such a way that the vortex cores wind adiabatically around one another according to a specific pattern. (The adiabatic condition here corresponds to demanding that any change in the position of each waveguide as a function of z occur on length scales much larger than the inverse photonic bandgap.) In one lattice, the waveguide pattern executes a braid $\hat{B}_1\hat{B}_2$, while in the other, the waveguide pattern implements the braid $\hat{B}_2\hat{B}_1$. Interfering the light output from the two lattices reveals the defining feature of non-Abelian braiding, namely that performing the same braids in different orders yields different results. We now proceed through each stage of the interferometer setup.

We start with the input stage of the PNAI. We assume

that the input light comes from three monochromatic, coherent laser sources, each focused on the core of a single vortex so that there is large overlap with the zero modes. Each of the three input beams is split by a 50/50 dielectric beam splitter, so that the light entering each vortex core comes from the same source beam. We will denote the light entering the upper branch of the interferometer in Fig. 2 as $|\lambda_1, \lambda_2, \lambda_3\rangle$, and $|\tilde{\lambda}_1, \tilde{\lambda}_2, \tilde{\lambda}_3\rangle$ for the lower branch. (The first beam splitter enforces the phase relation $\tilde{\lambda}_j = -i\,\lambda_j$.)

For the braiding stage of the interferometer, we choose, for example, $\hat{B}_1 = \hat{\tau}_2\hat{\tau}_1$ and $\hat{B}_2 = \hat{\tau}_2\hat{\tau}_1^{-1}\hat{\tau}_2\hat{\tau}_1^{-1}$ (see Fig. 2), which ensures that the vortices on the output facets of both lattices are in the same order. [38] In the SM, we provide more information about how to write these braiding patterns into the waveguide array. The output states from the two braids are

$$\hat{B}_1\hat{B}_2\,|\lambda_1, \lambda_2, \lambda_3\rangle = |-\lambda_1, \lambda_2, -\lambda_3\rangle \tag{15}$$

and

$$\hat{B}_2\hat{B}_1\,|\tilde{\lambda}_1, \tilde{\lambda}_2, \tilde{\lambda}_3\rangle = |-\tilde{\lambda}_1, -\tilde{\lambda}_2, \tilde{\lambda}_3\rangle. \tag{16}$$

In the final stage of the interferometer, the output beams from the braiding stage are combined at another beam splitter. The sign differences between the coherent states exiting the two branches of the interferometer cause the light to interfere constructively at one detector and destructively at the other. Which detector this is for each vortex depends on the relative signs of λ_i and $\tilde{\lambda}_i$, which in turn depend on the braids (see Fig. 2, and SM for more details). Since the effects of dynamical phases can be heavily suppressed in a controlled manner, as discussed earlier, the only source of this interference is the noncommutativity of braiding the vortices.

In summary, we have demonstrated in this paper a means to realize photonic analogues of topological zero modes in photonic lattices. We demonstrated that these "topological guided modes" can be understood at both the quantum and classical levels when the photons in the waveguide array are weakly interacting. We further proposed a photonic non-Abelian interferometer, feasible with current technology, to detect unambiguous signatures of the non-Abelian Berry phases that result from braiding these topological guided modes.

We thank Luca Dal Negro for inspiring discussions, and Chang-Yu Hou, Christopher Mudry, Titus Neupert, and Luiz H. Santos for valuable feedback on the manuscript. T.I. was supported by the National Science Foundation Graduate Research Fellowship Program under Grant No. DGE-1247312, and C.C. was supported by DOE Grant DEF-06ER46316.

[1] S. Pancharatnam, Proc. Ind. Acad. Sci. A **44**, 247 (1956).
[2] M. Berry, Proc. R. Soc. Lond. A **392**, 45 (1984).
[3] M. Berry, J. Mod. Opt. **34**, 1401 (1987).
[4] M. Z. Hasan and C. L. Kane, Rev. Mod. Phys. **82**, 3045 (2010).
[5] O. Peleg, G. Bartal, B. Freedman, O. Manela, M. Segev, and D. N. Christodoulides, Phys. Rev. Lett. **98**, 103901 (2007).
[6] F. D. M. Haldane and S. Raghu, Phys. Rev. Lett. **100**, 013904 (2008).
[7] S. Raghu and F. D. M. Haldane, Phys. Rev. A **78**, 033834 (2008).
[8] Z. Wang, Y. Chong, J. Joannopoulos, and M. Soljačić, Nature (London) **461**, 772 (2009).
[9] A. Khanikaev, S. Mousavi, W.-K. Tse, M. Kargarian, A. MacDonald, and G. Shvets, Nature Mater. **12**, 233 (2013).
[10] Y. E. Kraus, Y. Lahini, Z. Ringel, M. Verbin, and O. Zilberberg, Phys. Rev. Lett. **109**, 106402 (2012).
[11] M. C. Rechtsman, J. M. Zeuner, Y. Plotnik, Y. Lumer, D. Podolsky, F. Dreisow, S. Nolte, M. Segev, and A. Szameit, Nature (London) **496**, 196 (2013).
[12] L. Lu, L. Fu, J. Joannopoulos, and M. Soljačić, Nature Photon. **7**, 294 (2013).
[13] L. Lu, J. Joannopoulos, and M. Soljačić, Nature Photon. **8**, 821 (2014).
[14] E. Prodan and C. Prodan, Phys. Rev. Lett. **103**, 248101 (2009).
[15] N. Berg, K. Joel, M. Koolyk, and E. Prodan, Phys. Rev. E **83**, 021913 (2011).
[16] C. Kane and T. Lubensky, Nat. Phys. **10**, 39 (2014).
[17] H.C. Po, Y. Bahri, and A. Vishwanath, arXiv:1410.1320.
[18] R. Süsstrunk and S. Huber, Science **349**, 47 (2015).
[19] P. Wang, L. Lu, and K. Bertoldi, Phys. Rev. Lett **115**, 104302 (2015).
[20] F. Wilczek and A. Zee, Phys. Rev. Lett. **52**, 2111 (1984).
[21] R. Jackiw and C. Rebbi, Phys. Rev. D **13**, 3398 (1976).
[22] R. Jackiw and P. Rossi, Nuclear Physics B **190**, 681 (1981).
[23] W. P. Su, J. R. Schrieffer, and A. J. Heeger, Phys. Rev. Lett. **42**, 1698 (1979).
[24] C.-Y. Hou, C. Chamon, and C. Mudry, Phys. Rev. Lett. **98**, 186809 (2007).
[25] N. Read and D. Green, Phys. Rev. B **61**, 10267 (2000).
[26] D. A. Ivanov, Phys. Rev. Lett. **86**, 268 (2001).
[27] A. Y. Kitaev, Physics-Uspekhi **44**, 131 (2001).
[28] A. Stern, F. von Oppen, and E. Mariani, Phys. Rev. B **70**, 205338 (2004).
[29] A. Szameit and S. Nolte, Journal of Physics B: Atomic, Molecular and Optical Physics **43**, 163001 (2010).
[30] F. Lederer, G. I. Stegeman, D. N. Christodoulides, G. Assanto, M. Segev, and Y. Silberberg, Physics Reports **463**, 1 (2008).
[31] K. M. Davis, K. Miura, N. Sugimoto, and K. Hirao, Opt. Lett. **21**, 1729 (1996).
[32] O. Bahat-Treidel, O. Peleg, and M. Segev, Opt. Lett. **33**, 2251 (2008).

[33] M. C. Rechtsman, J. M. Zeuner, A. Tünnermann, S. Nolte, M. Segev, and A. Szameit, Nature Photonics **7**, 153 (2012).
[34] S. Mukherjee, A. Spracklen, D. Choudhury, N. Goldman, P. Öhberg, E. Andersson, and R. R. Thomson, Phys. Rev. Lett. **114**, 245504 (2015).
[35] W. Vogel and D.-G. Welsch, Quantum Optics (Wiley-VCH, Weinheim, GER, 2006).
[36] S. Yasui, K. Itakura, and M. Nitta, Nuclear Physics B **859**, 261 (2012).
[37] C. Nayak, S. H. Simon, A. Stern, M. Freedman, and S. Das Sarma, Rev. Mod. Phys. **80**, 1083 (2008).
[38] Of course, this is not the only braid we could have chosen. For example, the choice $\hat{B}_1 = \hat{\tau}_1\hat{\tau}_2$ and $\hat{B}_2 = \hat{\tau}_2\hat{\tau}_1$ also satisfies the requirement that vortices end up in the same order in both braids.